

Article

Determination of Pipeline Leaks Based on the Analysis the Hurst Exponent of Acoustic Signals

Ayrat Zagretdinov *, Shamil Ziganshin , Yuri Vankov, Eugenia Izmailova and Alexander Kondratiev

Department of Industrial Heat Power and Heat Supply Systems, Kazan State Power Engineering University, Kazan 420066, Russia

* Correspondence: azagretdinov@yandex.ru

Abstract: Currently, acoustic methods are widely used as a way to detect pipeline leaks. This is due to the fact that the acoustic signal has sufficiently capacious information about the state of the pipeline. The effectiveness of acoustic monitoring depends on the correct extraction of this information from the diagnostic signal. Currently, there is a search for new, more effective methods for analyzing acoustic signals. The article proposes to apply the theory of fractals to determine pipeline leaks. One of the most accurate methods for determining the fractal dimension of time series is R/S analysis using the Hurst exponent. An experimental stand has been developed and created, which includes a steel pipeline with water circulating in it. Water leakage from the pipeline was simulated by installing discs with holes of different diameters. The discs were placed in a special fitting on the surface of the pipeline. Acoustic signals recorded from the pipeline surface at different leakages and water pressure were analyzed. A relationship has been established between the size of the leak and the Hurst exponent of acoustic signals. The proposed method is compared with spectral analysis. Empirical experience has proven that R/S analysis can be used to determine pipeline leaks, as well as their classification by size.



Citation: Zagretdinov, A.; Ziganshin, S.; Vankov, Y.; Izmailova, E.; Kondratiev, A. Determination of Pipeline Leaks Based on the Analysis the Hurst Exponent of Acoustic Signals. *Water* **2022**, *14*, 3190. <https://doi.org/10.3390/w14193190>

Academic Editors: Gabriele Freni, Mariacrocetta Sambito and Enrico Creaco

Received: 26 August 2022

Accepted: 6 October 2022

Published: 10 October 2022

Publisher's Note: MDPI stays neutral with regard to jurisdictional claims in published maps and institutional affiliations.



Copyright: © 2022 by the authors. Licensee MDPI, Basel, Switzerland. This article is an open access article distributed under the terms and conditions of the Creative Commons Attribution (CC BY) license (<https://creativecommons.org/licenses/by/4.0/>).

Keywords: pipeline; leakage; fractals; Hurst exponent; R/S analysis; acoustic control

1. Introduction

Pipeline systems are necessary to provide human populations, industry and agriculture with vital products: natural gas, oil products, heat carriers (hot water and steam), air, drinking and process water, etc. In the Russian Federation alone, the length of pipeline networks exceeds 5 million km.

The long length of pipeline networks and their high degree of deterioration lead to leaks. For example, in Hong Kong, water losses due to leaks are approximately 15%, in Europe approximately 20% of the total transported water [1], and in cities such as Dublin (Ireland), Lusaka (Zambia) and Kolkata (India) can reach up to 40–60% [2].

Hidden leaks pose a big problem for networks. Latent leaks are losses of water (or other liquid product), which do not manifest in bursting out to the surface or the flooding of various underground utilities. This determines the difficulty of finding them and leads to significant losses of energy carrier capacity.

Accidents in pipeline systems, as well as illegal tie-ins with the aim of stealing the transported product, lead not only to significant economic damage, but can also create the risk of landslides, fires, explosions or environmental pollution.

In this regard, the need to improve the quality and reliability of pipeline systems is an urgent problem. Today, there are many methods for locating the depressurization of pipelines, including the visual-optical method, electromagnetic control, acoustic control, ultrasonic control, radiographic examination, thermographic testing, hydro- or pneumatic testing with pressure measurement before and after the leak, etc. [3–18]. However, despite the variety of control methods, it is impossible to single out one that is effective in all conditions [4].

From research authors [4,19], it can be concluded that acoustic methods are the most balanced in comparison with others. This is due to the fact that the acoustic signal has sufficient information about the state of the pipeline. As a method of assessing the condition of pipelines, acoustic methods have been used for a long time [4,20–29]. The main problem of the effective use of acoustic control is the need for high-quality extraction of the information from the signal.

Initially, scientists used the Fourier transform to process acoustic signals [27]. Undoubtedly, this is not enough. The Fourier transform inherently cannot distinguish a stationary signal from a non-stationary one, which is a big problem for its applicability. This problem can be partially solved by the windowed Fourier transform, which can characterize the distribution of the signal frequency (with amplitude) over time. The main problem with its use, however, is the Heisenberg uncertainty principle, which arises for the parameters of the time and frequency of the signal. This uncertainty principle is based on the fact that it is impossible to know exactly what frequency is present in the signal at a given time (we can only determine the frequency range). It is also impossible to know at what point in time the frequency is present in the signal (we can only determine the period of time). In this regard, the windowed Fourier transform cannot fully resolve the signal problem.

With ongoing developments in science and technology, more advanced processing methods have begun to be used to analyze the acoustic signal.

Two relatively new methods of the mathematical processing of vibration signals are the wavelet transform and the Hilbert–Huang transform, which have recently become widely used in practice [29–31]. These transformations allow us to solve the Heisenberg uncertainty problem. The main disadvantage of wavelet analysis, however, is associated with the need to choose a basic wavelet depending on the nature of the initial time series. In the process of analyzing non-stationary signals, information about the main basis, as a rule, is not available, and for this reason, it becomes necessary to select possible options to obtain optimal results.

The Hilbert–Huang transform does not require the choice of the basis function. However, this method does not have a rigorous theoretical basis. It requires additional research to confirm the legitimacy of its application in each specific case. In addition, the disadvantages associated with having to choose splines for decomposition, the stopping criterion when filtering out the remainder, the significant modes, mixing of modes, and edge effects increase the complexity and complicate the interpretation of the results.

Methods for analyzing signals are carried out in various ways. One of these methods is the theory of artificial neural networks. The mathematical apparatus of neural networks improves the accuracy of the diagnostic process due to the existing knowledge base about the operation of analogues. The disadvantages include the complexity of the implementation and training of the neural network. In addition, it is worth highlighting the low degree of unification (for each new object, it is necessary to create a new network and then train it) [4,32,33].

Currently, there is an active testing of non-traditional approaches in the processing and analysis of information. The theory of fractals is one of the most promising areas of mathematical data processing. The concept of a fractal is associated with geometric objects that satisfy such a criterion as self-similarity. Fractals have a rough or fragmented geometric shape that can be divided into parts, each of which is a reduced semblance of the whole. To describe fractal structures based on a quantitative assessment of their complexity, a coefficient called fractal dimension is used. One of the most accurate methods for determining the fractal dimension of a time series is R/S analysis using the Hurst exponent.

Fractal theory is widely used in medicine, technology, meteorology, finance, and many other industries. For example, work [34] presents the use of fractals for the early diagnosis of breast cancer, where the fractal dimension and the Hurst exponent are used to determine the location of microcalcifications on a mammogram. In [35], the fractal dimension of magnetic resonance imaging data was used to diagnose a brain tumor. In a

study [36], the fractal dimension of fluctuations in brain oxygen demand revealed brain abnormalities in autism spectrum disorder. The authors of [37] used the fractal analysis of vibroacoustic signals for express diagnostics of the traction drives of electric trains. In [38], the authors show that the Hurst exponent of a time series can be used as an indicator of the predictability of precipitation. The work in [39] proposes a prediction methodology based on the analysis of the Hurst exponent for the process of rolling bearing degradation.

We see the possibility of successful application of the theory of fractals to control the technical condition of pipelines. Inside pipeline systems, there is a movement of liquid or gas, and there are always complex disordered vibrations, which are denoted by the term “noise”. From the point of view of classical methods of signal analysis, such oscillatory processes do not carry useful information. However, such signals have signs of self-similarity which can be estimated by the fractal dimension. The use of fractal analysis will not only detect the leak, but also classify it by size.

The purpose of this work is to consider the possibility of using R/S analysis to determine pipeline leaks, as well as their classification by size. For this purpose, studies were carried out on an experimental stand where steel pipeline leaks were simulated at various water flow parameters. Acoustic signals were recorded using a sensor that allows measuring longitudinal and radial vibrations of the pipe wall. The Hurst exponent was calculated for each signal, and the pipeline defect was estimated along the boundary of the confidence interval.

2. Materials and Methods

R/S analysis was developed by hydrologist H.E. Hurst [40]. Hurst’s statistical model was created on the basis of Einstein’s work on Brownian motion, which is a model of the chaotic motions of particles. The essence of the theory is that the distance R that a particle travels increases in proportion to the square root of the time T :

$$R = T^{0.5} \quad (1)$$

Hurst completed the Einstein calculation and brought it to the main form:

$$R/S = c \times n^H \quad (2)$$

where R is the normalized range of variation, S is the standard deviation, c is a constant, n is the number of sample elements, and H is the Hurst exponent.

If the process is random, then the Hurst exponent $H = 0.5$. In the process of studying the dynamics of the ebb and flow of the Nile River, Hurst found that $0.5 < H < 1$. This means that the normalized range changes faster than the square root of time, i.e., the system travels a greater distance than the probabilistic process. This process is called persistent and is characterized by long-term memory; subsequent indicators are highly dependent on the past. Close to this is the sensitivity to initial conditions characteristic of chaos. The Hurst exponent $0 < H < 0.5$ means antipersistent process. Under such conditions, the system is qualified by abundant but minor changes. The antipersistent process changes more intensively than the involuntary one and is typical for turbulence effects.

B. Mandelbrot, who discovered fractal geometry, found in the Hurst formula laws that are associated with the fractality of a time series. The Hurst exponent is connected with the Hausdorff–Besicovitch dimension (fractal dimension) as follows:

$$D = 2 - H \quad (3)$$

2.1. R/S Analysis Algorithm

Let there be a sample of n elements, which is a time series. The algorithm for performing R/S analysis is as follows [41].

1. The smallest own divisor m of the sample n is determined. Sample n is divided into $k = n/m$ groups.

It should be noted that the number of elements of each group is equal to m . Elements in each group will be designated as t_i .

- For each group, the average is calculated

$$\bar{t}_k = \frac{1}{m} \sum_{i=1}^m t_i, \frac{1}{m} \sum_{i=m+1}^{2m} t_i \dots \frac{1}{m} \sum_{i=(k-1)m+1}^n t_i \quad (4)$$

and accumulated deviations from the mean X_i

$$X_1 = t_1 - \frac{1}{m} \sum_{i=1}^m t_i, X_2 = t_2 - \frac{1}{m} \sum_{i=1}^m t_i + X_1 \dots X_m = t_m - \frac{1}{m} \sum_{i=1}^m t_i + X_{m-1} \quad (5)$$

- Calculate the normalized diaposon for each group

$$R_k = \max(X_i) - \min(X_i) \quad (6)$$

- For each group, the standard deviation S_k calculated according to the standard formula

$$S_k = \sqrt{\frac{1}{m} \sum_{i=1}^m (t_i - \bar{t}_k)^2} \quad (7)$$

- The R/S index for each group is defined as R_k/S_k . Then, the average range of the variation is found

$$\overline{R/S_j} = \frac{1}{k} \sum_{i=1}^k \frac{R}{S_i} \quad (8)$$

The index j in this instance means that the average range change obtained at j -th step, which conform to the j -th proper divisor.

- The procedure described above is repeated for all possible proper divisors as m . At the last step, $m = n/2$.

Thus, a selection is obtained $\overline{R/S_j}$

The number of elements in the sample match the number of proper divisors.

- A graph of dependences of $\log R/S$ on $\log m$ is being built and using the method of least squares a regression equation of the form

$$\log R/S = H \times \log m + \log c \quad (9)$$

where H is the Hurst exponent.

To calculate the Hurst exponent in the LabView programming environment, the FractLab-1 program was developed.

2.2. Experimental Stand

To study the possibility of using the considered algorithm for solving the problem of determining pipeline leaks, an experimental stand was developed and created.

The scheme of the experimental device is shown in Figure 1.

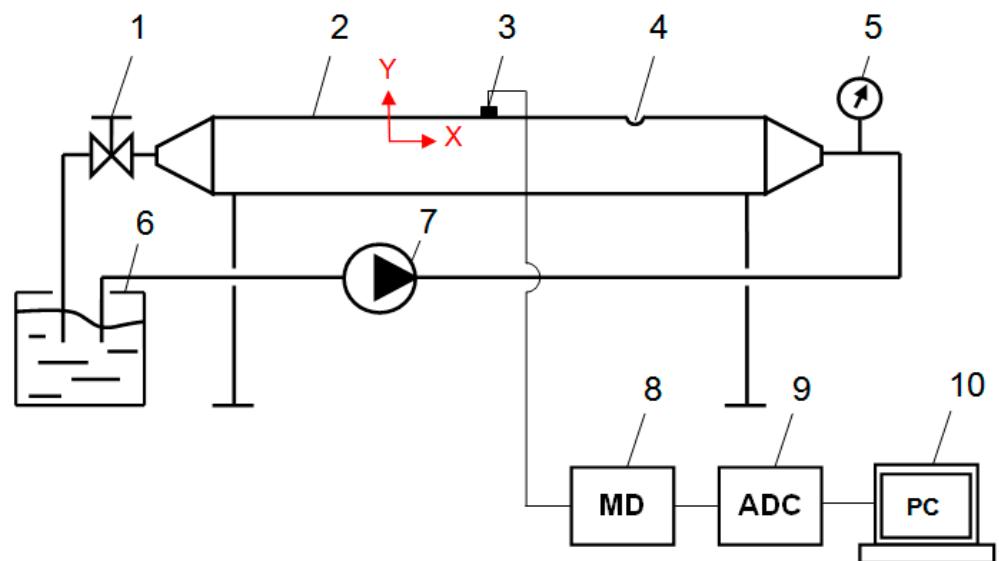


Figure 1. Experimental device: 1—valve; 2—pipeline (length 2 m, external diameter 0.159 m, wall thickness 6 mm); 3—vibration acceleration sensor AR2038R; 4—defect; 5—manometer; 6—capacity; 7—pump LEO XKJ-900 I; 8—matching device AG01-3; 9—analog-to-digital converter NI USB-6229; 10—computer.

The experimental stand is a closed loop with circulating water. By closing valve—1, the pump discharge pressure was regulated in the range of 1.5–3.5 bar in 0.5 bar increments. The pressure was controlled using a pressure gauge—5.

According to the hydraulic characteristics of the pump and the readings of the pressure gauge, its performance was established (Table 1).

Table 1. Dependence of pump performance on discharge pressure.

Pressure, Bar	Consumption, L/Min
1.5	45
2	38
2.5	31
3	24
3.5	16

Acoustic vibrations of pipeline 2 were recorded by piezoelectric sensor 3 (AP2038R—manufacturer GlobalTest), which was installed after the defect in the direction of fluid flow (Figure 1). The vibration sensor has the following characteristics: axial sensitivity 100 mV/g; amplitude range ± 50 g; maximum shock ± 500 g; and natural frequency 35 kHz. The excellence of such a sensor is the simultaneous meterage of the signal at one vibration point along different coordinate axes.

Acoustic vibrations were investigated in the longitudinal and transverse directions relative to the pipeline axis (in Figure 1, directions X and Y, respectively). For the registration and analysis of signals, an original software packet written in the LabView environment was used [4]. The sampling frequency of the analog-to-digital converter—9 is taken to be 44.1 kHz.

As models of pipeline defects, we used disks with holes of different diameters (from 1 to 8 mm), shown in Figure 2. The disks were installed and clamped on a fitting welded to the pipe (Figure 3).



Figure 2. Discs with holes of different diameters.



Figure 3. Method of fixing discs on the pipeline: (a) side view, (b) top view.

3. Results and Discussion

The experiment was carried out according to the following algorithm. A disk with a hole of a certain diameter was installed on the pipe, which simulated a leak. By turning on the pump and opening the valve in the pipe, the required pressure was created (from 1.5 to 3.5 bar in 0.5 bar increments). At each pump discharge pressure, acoustic signals were recorded into the computer memory. Then, the disk with the hole was changed to the next one and the algorithm was repeated.

With large diameters of the defect, it was not possible to create a high pump discharge pressure due to a decrease in the hydraulic resistance of the pipe caused by a large fluid leak. Table 2 shows the maximum pump discharge pressures for different bore diameters.

Table 2. Maximum pump discharge pressure at different bore diameters.

Hole Diameter, Mm	Maximum Pressure, Bar
1	3.5
2	3.5
3	3
4	2.5
5	2.5
6	2
7	2
8	2

A pipe with a disc without a hole installed in the fitting is accepted as defect-free.

Signals with a length of 20,000 counts were analyzed, while the Hurst exponent was calculated in the interval $\log m = 3.32 \div 10$. A typical acoustic signal of a pipe with water movement and a Hurst dependence plot for it are shown in Figure 4.

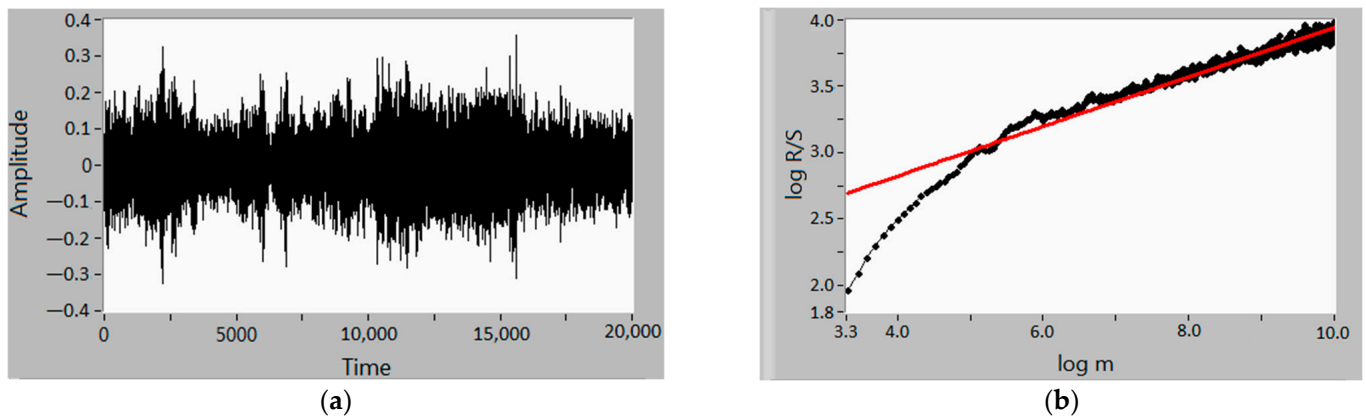


Figure 4. Acoustic signal (a) and Hurst dependence graph (b, red line—regression graph).

To analyze the results of experimental studies, an approach typical for anomaly rejection procedures was used. For the set of calculated values of the Hurst exponent, the following algorithm was used.

1. The position estimate is calculated \bar{H} .
2. The spread estimate S is calculated as a standard deviation.
3. For a given significance level α confidence interval is constructed:

$$\bar{H} + S \times t\left(1 - \frac{\alpha}{2}, m - 2\right)$$

where $t(\alpha, m)$ is the α -quantile of the Student’s distribution with m degrees of freedom.

Based on the acoustic signals of a defect-free pipe, obtained at different hydraulic loading, a confidence interval was formed with a significance level of 0.01 (Figure 5).

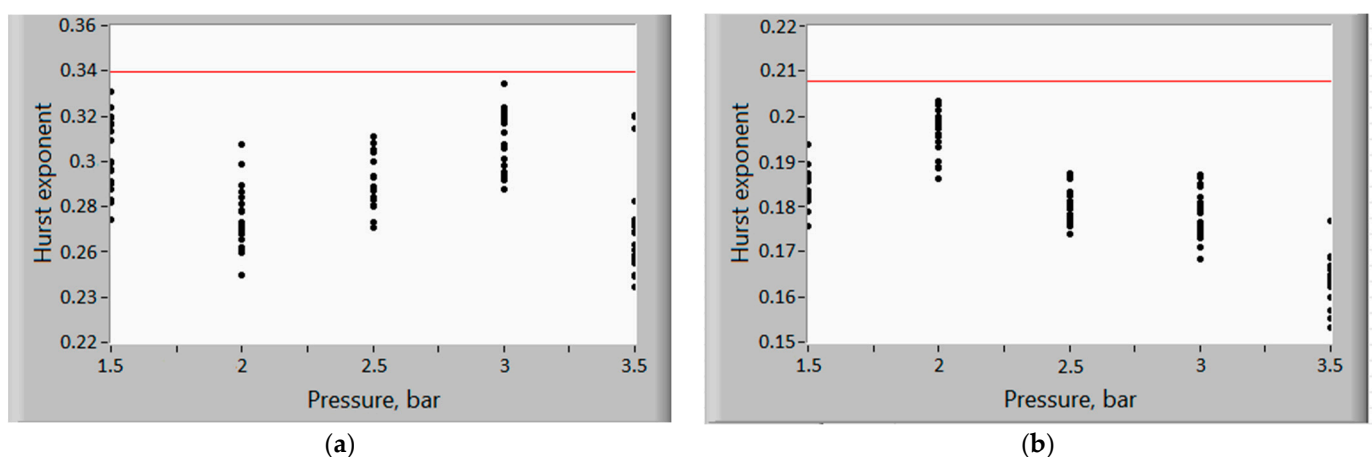


Figure 5. Formation of the confidence interval: (a) for X-axis signals, (b) for Y-axis signals.

The border of the confidence interval is shown with a red line. For signals recorded along different axes, their own confidence interval was formed (Figure 5a—along the X axis, Figure 5b—along the Y axis), due to the fact that the values of the Hurst exponent for different axes differ significantly. As can be seen from the graphs, the Hurst exponent at different pressures in the absence of a leak in the pipe is approximately at the same level.

Acoustic signals are antipersistent, which indicates the presence of a turbulent flow. This assumption is confirmed by calculations of the Reynolds number (Table 3) according to the well-known formula:

$$Re = \frac{w \times D}{\nu}$$

where w is the water flow rate, m/s, D is the pipe diameter, m, ν is the kinematic viscosity of water, m²/s.

Table 3. The results of calculating the Reynolds number for different modes of water flow in the pipe.

Pressure, Bar	Reynolds Number
1.5	6461
2	5456
2.5	4451
3	3446
3.5	2441

Figures 6–10 show the dependence of the Hurst exponent on the diameter of the defect at different pump discharge pressures. Unlike X-axis signals, Y-axis signals always remain antipersistent (i.e., the Hurst exponent for them is $H < 0.5$).

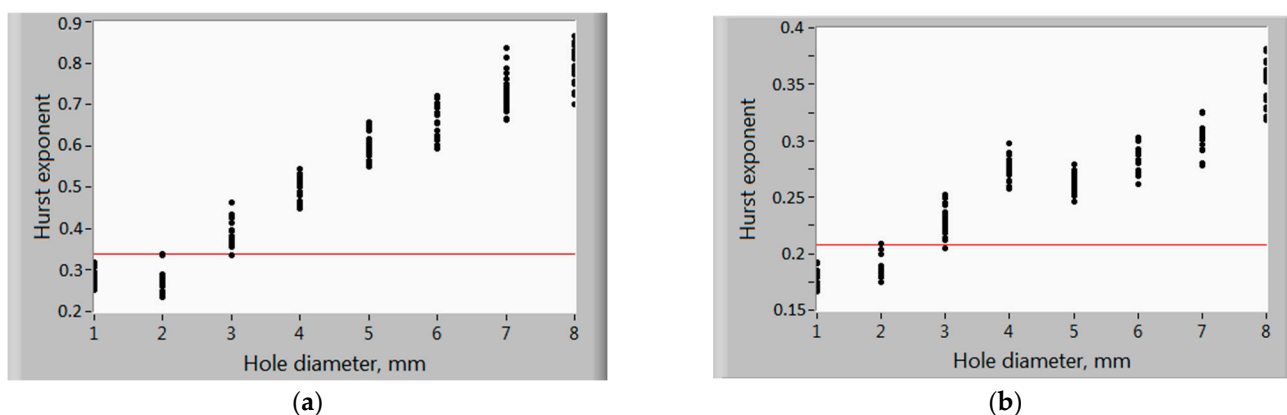


Figure 6. Values of the Hurst exponent at a pump discharge pressure of 1.5 bar: (a) for X-axis signals, (b) for Y-axis signals.

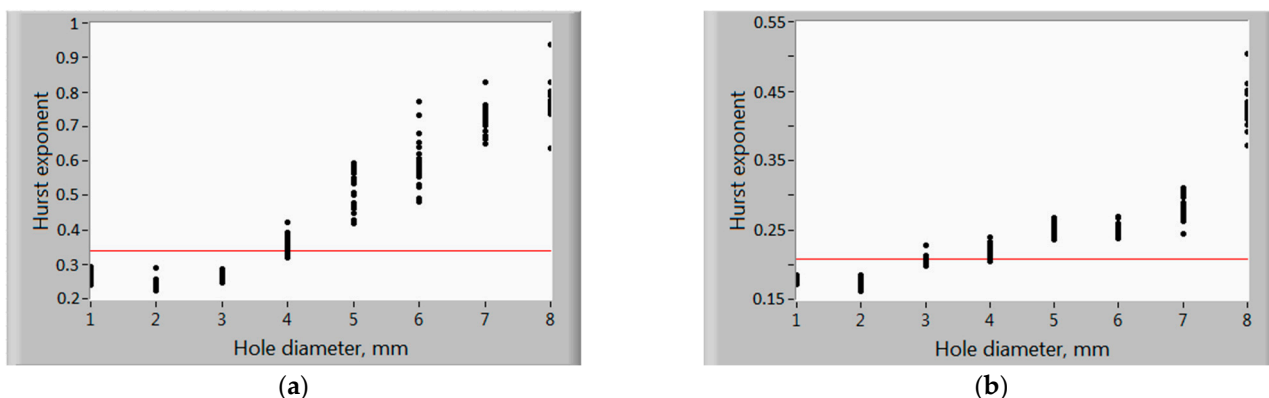


Figure 7. Values of the Hurst exponent at a pump discharge pressure of 2 bar: (a) for X-axis signals, (b) for Y-axis signals.

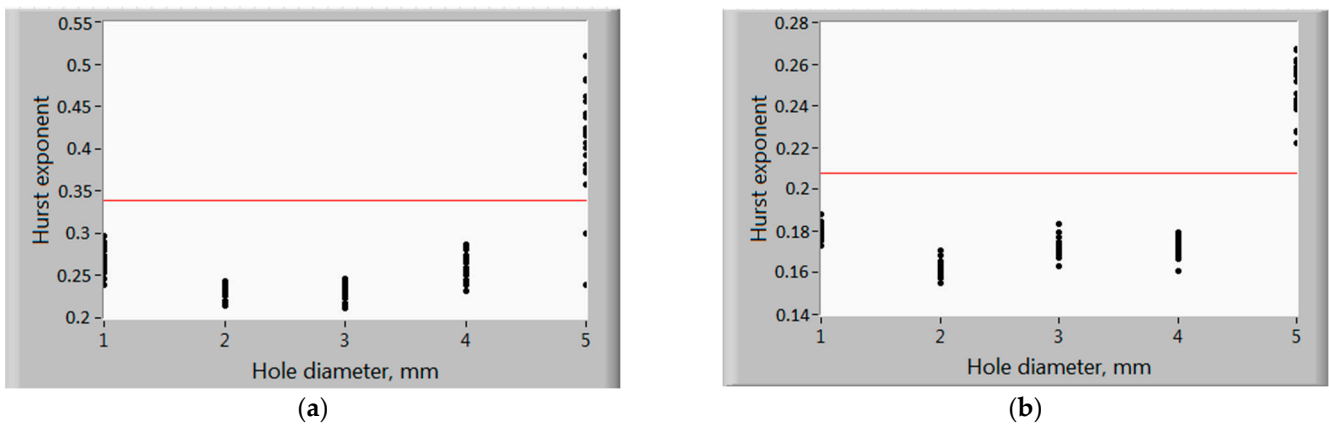


Figure 8. Values of the Hurst exponent at a pump discharge pressure of 2.5 bar: (a) for X-axis signals, (b) for Y-axis signals.

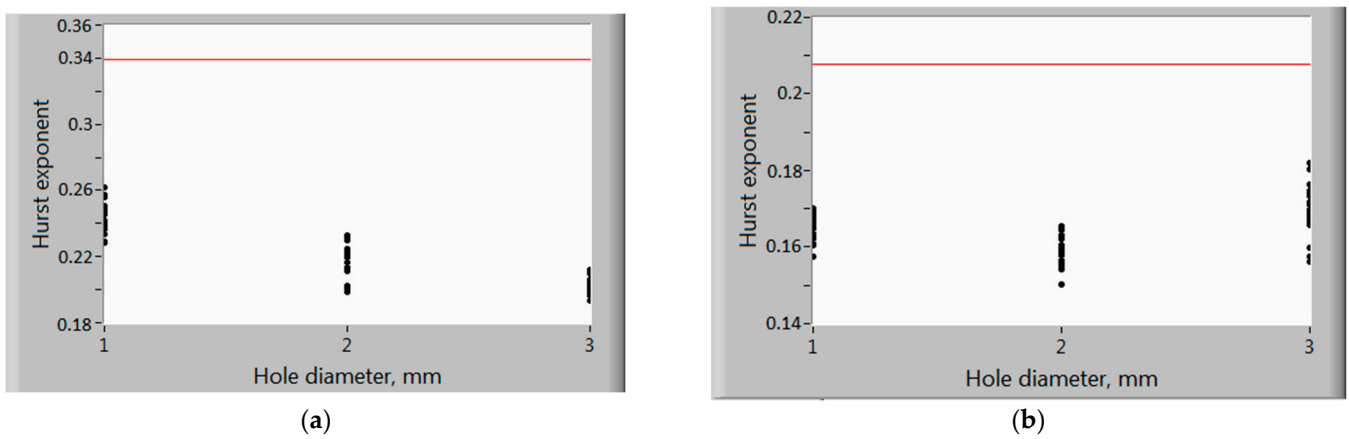


Figure 9. Values of the Hurst exponent at a pump discharge pressure of 3 bar: (a) for X-axis signals, (b) for Y-axis signals.

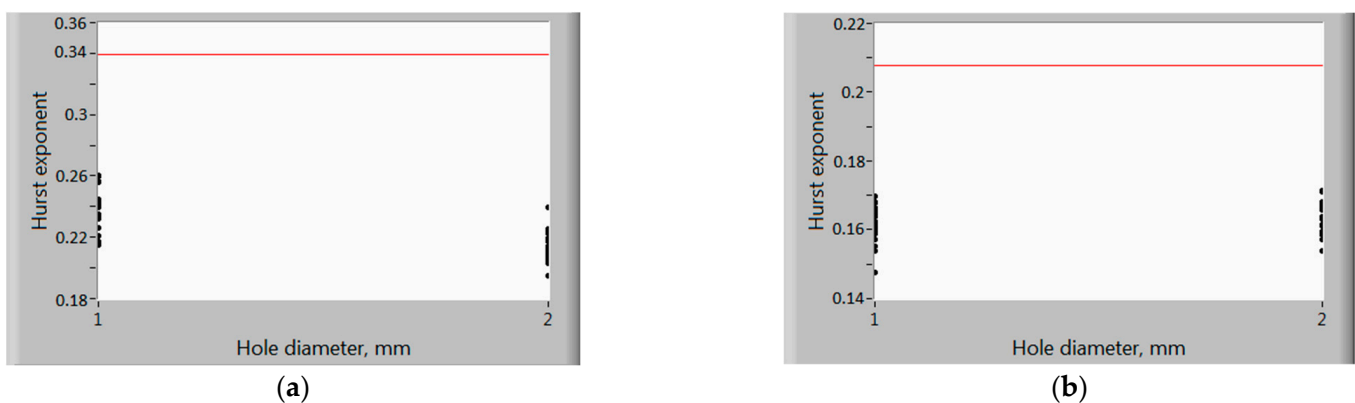


Figure 10. Values of the Hurst exponent at a pump discharge pressure of 3.5 bar: (a) for X-axis signals, (b) for Y-axis signals.

Figure 6 shows that at a water pressure in the pipe of 1.5 bar, defects less than 3 mm are not detected because the Hurst exponent H for them lies within the confidence interval. With an increase in the size of the defect, the degree of turbulence of the flow decreases, therefore, the Hurst exponent increases and with large leaks tends to the level of the deterministic signal (to the level $H = 1$).

At a pressure of 2 bar (Figure 7), the sensitivity of the control decreased; defects of 3 mm or less are not detected. According to our assumption, this is due to an increase in the vortex formation of the flow.

With a further increase in pressure, a similar picture is observed. At a pressure of 2.5 bar, only a 5 mm defect is detected (Figure 8). It should be noted that, at such a pressure, defects of a larger diameter could not be considered (see Table 2).

The results presented in Figures 9 and 10 confirm the impossibility of detecting defects with a size of 3 mm or less at pressures of 3 and 3.5 bar.

We will compare the proposed method with standard spectral analysis.

In Figure 11, the spectra of defect-free and defective pipelines at a pressure of 2 bar are superimposed on each other. The normalization procedure was applied to the spectra. Normalization refers to the separation of each spectral component by the maximum amplitude of the spectrum.

Figure 11 shows that with small leaks in the pipeline (with defects from 1 to 5 mm), the amplitude of high-frequency oscillations increases (over 15 kHz). The mechanism of generating high frequencies is explained by the high leakage rate at small defect sizes. High speed leads to the appearance of the cavitation effect (the formation of minute shock waves) [42]. With large sizes of defects, fluctuations at low frequencies (up to 6 kHz) are characteristic. In this regard, the choice of the optimal frequency range for spectral analysis of leakage signals is difficult.

We compared the spectra of defective pipelines in different frequency ranges using the correlation coefficient. For this purpose, a reference spectrum was formed by averaging the spectra of a defect-free pipeline. Figure 12 shows the results of comparing the spectra with the reference. The median value of the correlation coefficient was obtained by comparing 20 spectra.

Figure 12 shows that the analysis of the statistical relationship between the spectra allows us to determine only the presence of a leak, but not its size.

Figure 13 shows the results of measuring spectra in the dB scale without normalization. To estimate the energy change in the frequency bands 0.02–6 kHz and 15–20 kHz, the spectral areas were calculated (by integrating the spectral curve). The calculation results are shown in Figure 14.

Figure 14 shows that as the defect size increases, the spectrum area first increases and then decreases. This is more noticeable in the high-frequency region. The decrease in acoustic energy with an increase in the size of the defect is consistent with the conclusions of the article [42].

It is difficult to estimate the size of the defect by the amplitude level, since this level is not known a priori in real conditions [43]. R/S analysis is not sensitive to changes in signal strength and is a promising method for classifying the size of leaks.

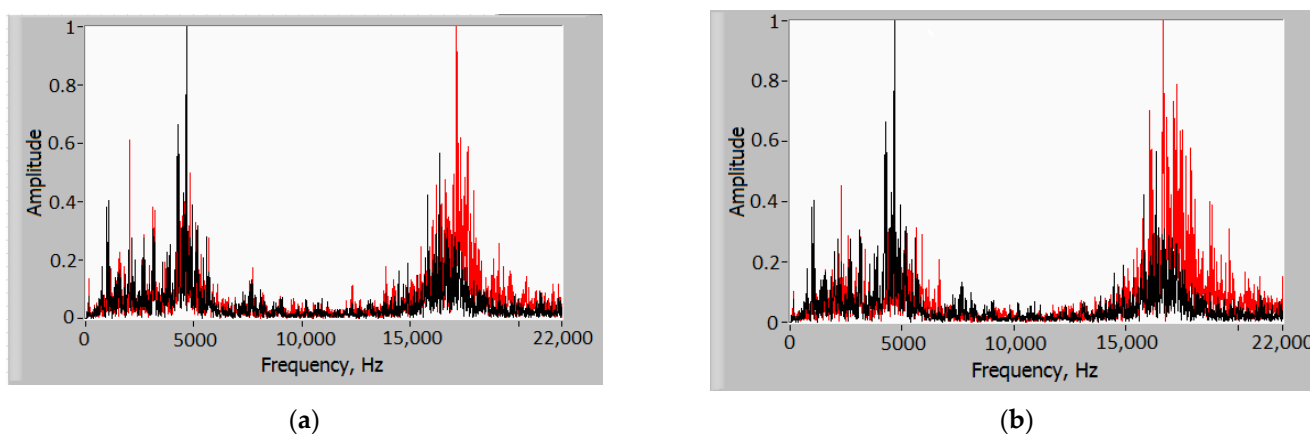


Figure 11. Cont.

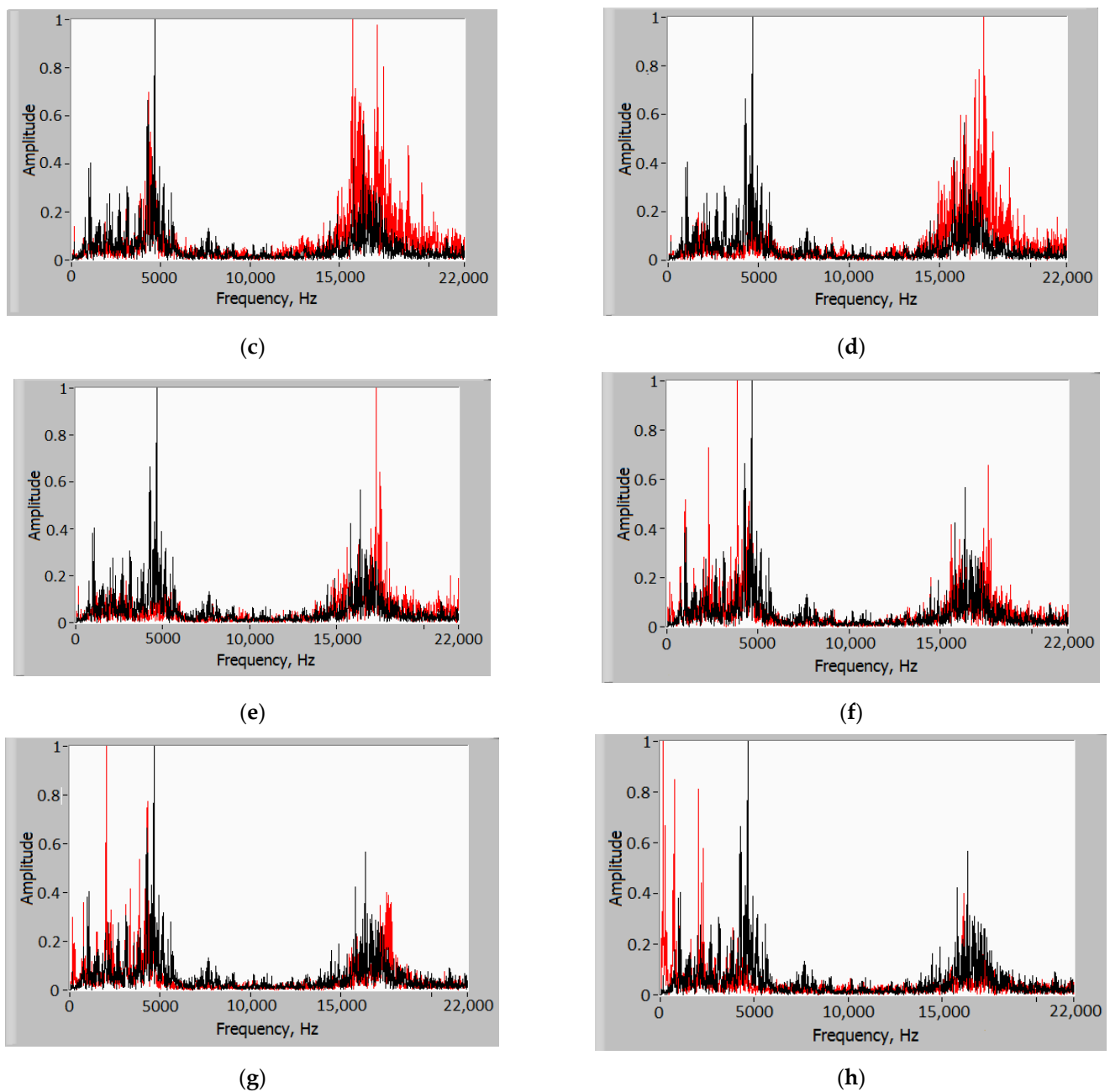


Figure 11. Comparison of the spectra of acoustic signals of the pipeline at a pressure of 2 bar (the spectrum of a defect-free pipeline is indicated in black; the spectrum of a pipeline with a leak is indicated in red): (a) for a defect diameter of 1 mm, (b) for a defect diameter of 2 mm, (c) for a defect diameter of 3 mm, (d) for a defect diameter of 4 mm, (e) for a defect diameter of 5 mm, (f) for a defect diameter of 6 mm, (g) for a defect diameter of 7 mm, (h) for a defect diameter of 8 mm.

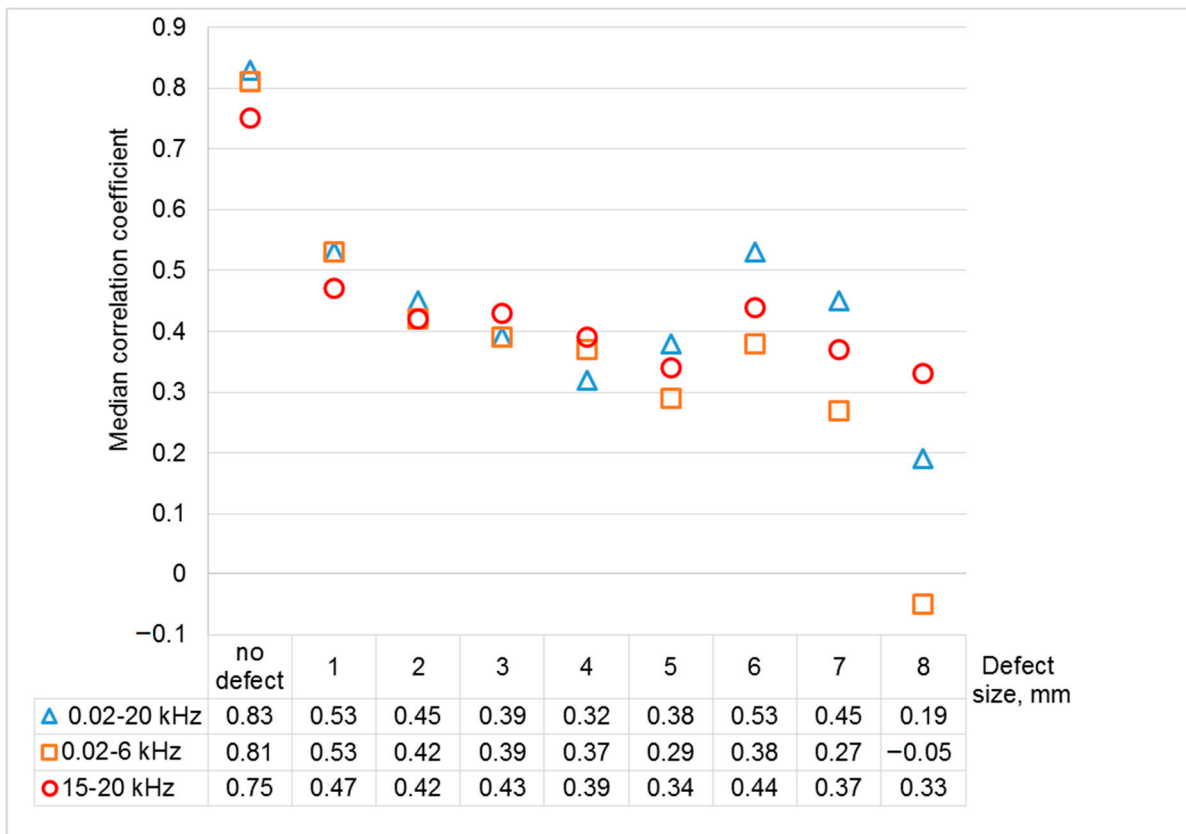
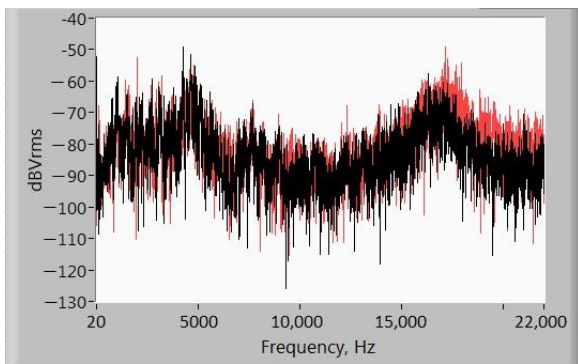
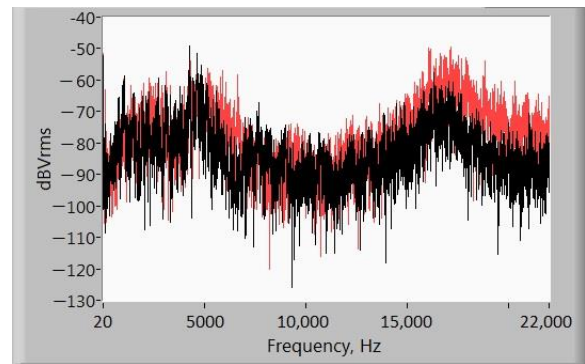


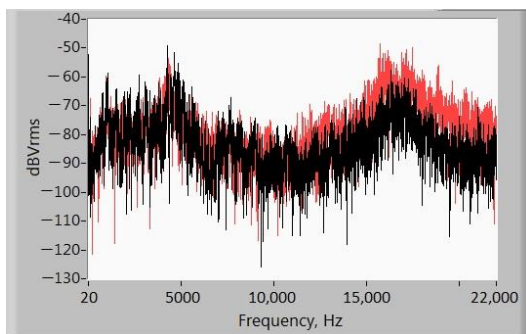
Figure 12. Correlation coefficients of acoustic spectra.



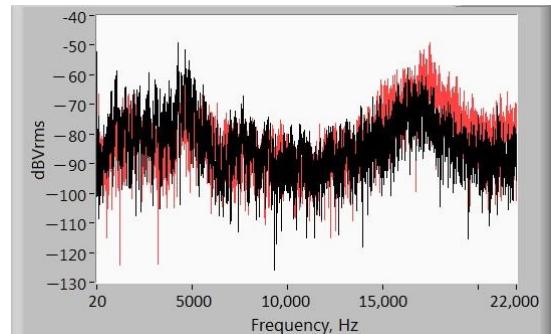
(a)



(b)



(c)



(d)

Figure 13. Cont.

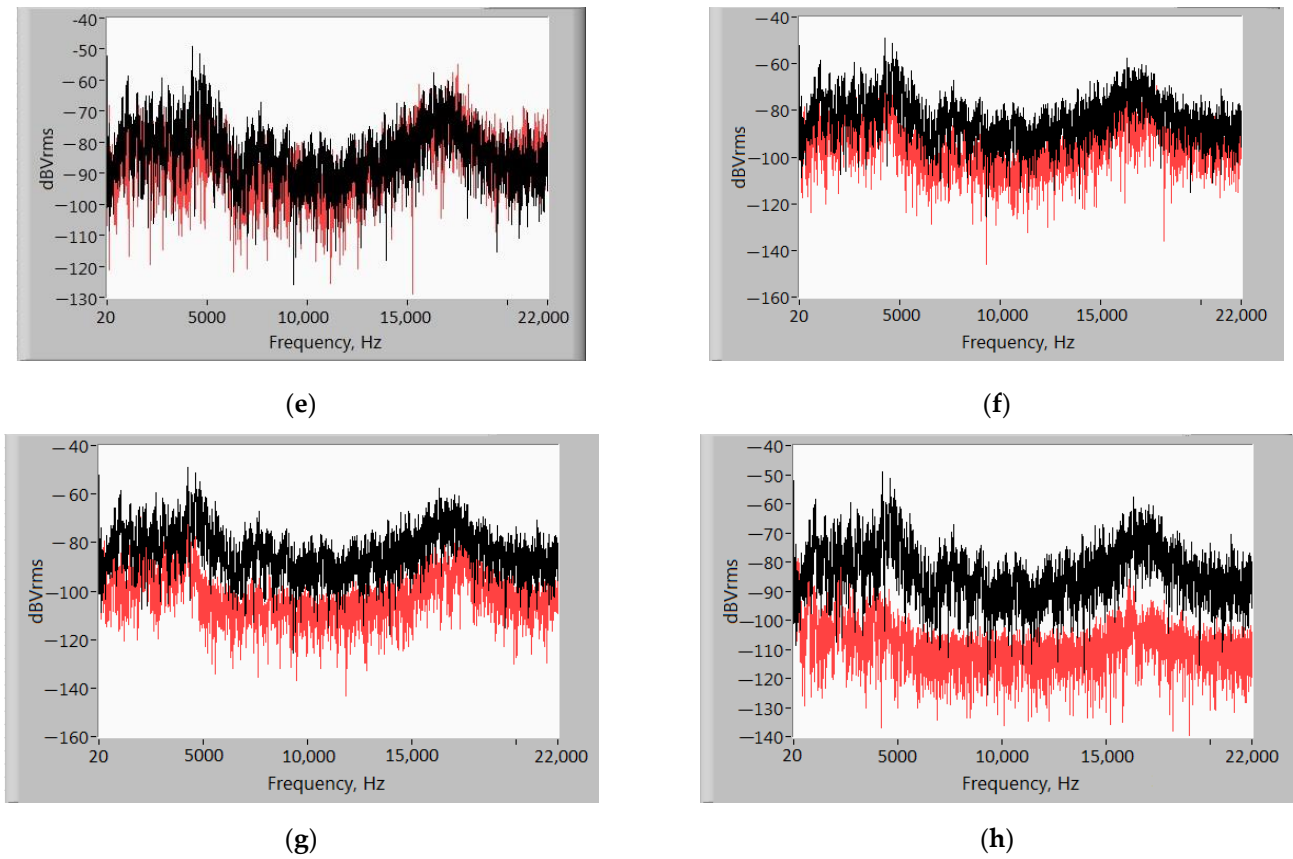


Figure 13. Spectra of acoustic signals of the pipeline at a pressure of 2 bar (the spectrum of a defect-free pipeline is indicated in black; the spectrum of a pipeline with a leak is indicated in red): (a) for a defect diameter of 1 mm, (b) for a defect diameter of 2 mm, (c) for a defect diameter of 3 mm, (d) for a defect diameter of 4 mm, (e) for a defect diameter of 5 mm, (f) for a defect diameter of 6 mm, (g) for a defect diameter of 7 mm, (h) for a defect diameter of 8 mm.

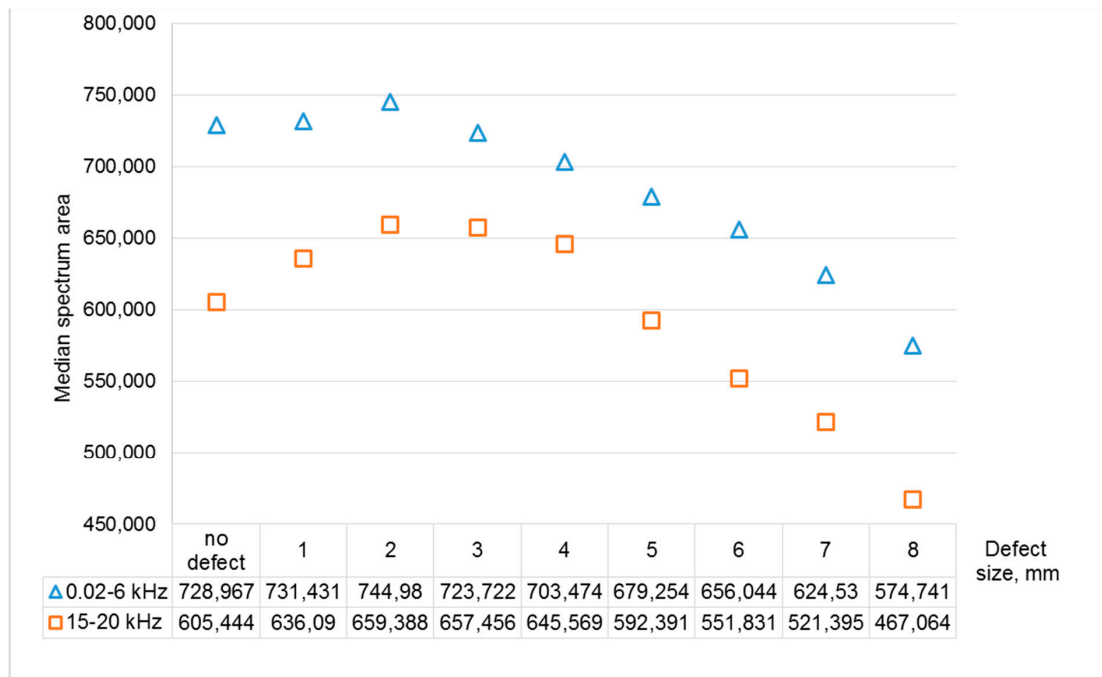


Figure 14. Results of calculations of the area of acoustic spectra.

4. Conclusions

A new approach to detecting leaks in pipeline systems is proposed. R/S analysis allows us to determine the degree of stochasticity of pipeline vibrations, which is directly related to the nature of the fluid flow in the pipe.

During the process of liquid flowing turbulently through a hole in the pipe wall, pulsations of liquid density occur. The appearance of such pulsations is manifested in the form of elastic waves in the liquid itself and in the walls of the pipe. The determining parameters of these pulsations are the flow rate of the liquid and the size of the hole. In addition, the presence of leaks leads to a change in the flow rate in the pipe itself.

With an increase in the size of the leak, the flow rates in the hole and in the pipeline decrease, which leads to a decrease in turbulence. In this case, the elastic vibrations of the pipeline wall acquire a deterministic character. The Hurst exponent allows for the identification of these changes in signals.

As the pressure inside the pipe increases, the sensitivity of the method to small leaks decreases. This is due to an increase in vortex formation, since the flow rate depends on the pressure drop at the inlet and outlet of the leak.

Undoubtedly, the method requires further research using CFD modeling to establish the scope of its effective application. However, based on the conducted research, an argument can be made for the high potential of using the proposed method for classifying leaks by size.

Author Contributions: Conceptualization, A.Z.; investigation, S.Z.; validation, Y.V.; writing - original draft preparation, E.I.; writing—review and editing, A.K. All authors have read and agreed to the published version of the manuscript.

Funding: This research was funded by the Russian Science Foundation grant No. 22-79-10045, <https://rscf.ru/en/project/22-79-10045/> (accessed date 10 October 2022).

Conflicts of Interest: The authors declare no conflict of interest.

References

1. Pan, B.; Duan, H.F.; Meniconi, S.; Brunone, B. FRF-based transient wave analysis for the viscoelastic parameters identification and leak detection in water-filled plastic pipes. *Mech. Syst. Signal Process.* **2021**, *146*, 107056. [[CrossRef](#)]
2. Cao, X.Q.; Ruan, C.M. Compilation of investigation on water loss rate of water supply pipelines in global major cities. *Water Purificat. Technol.* **2017**, *36*, 6–14.
3. Dindorf, R.; Wos, P. Universal programmable portable measurement device for diagnostics and monitoring of industrial fluid power systems. *Sensors* **2021**, *21*, 3440. [[CrossRef](#)] [[PubMed](#)]
4. Vankov, Y.; Romyantsev, A.; Ziganshin, S.; Politova, T.; Minyazev, R.; Zagretidinov, A. Assessment of the condition of pipelines using convolutional neural networks. *Energies* **2020**, *13*, 618. [[CrossRef](#)]
5. Hawari, A.; Alkadour, F.; Elmasry, M.; Zayed, T. A state of the art review on condition assessment models developed for sewer pipelines. *Eng. Appl. Artif. Intell.* **2020**, *93*, 103721. [[CrossRef](#)]
6. Siow, P.Y.; Ong, Z.C.; Khoo, S.Y.; Lim, K. Damage sensitive PCA-FRF feature in unsupervised machine learning for damage detection of plate-like structures. *Int. J. Struct. Stab. Dyn.* **2021**, *21*, 2150028. [[CrossRef](#)]
7. Pesinis, K.; Tee, K.F. Statistical model and structural reliability analysis for onshore gas transmission pipelines. *Eng. Fail. Anal.* **2017**, *82*, 1–15. [[CrossRef](#)]
8. Mazumder, R.K.; Salman, A.M.; Li, Y.; Yu, X. Reliability analysis of water distribution systems using physical probabilistic pipe failure method. *J. Water Resour. Plan. Manag.* **2019**, *145*, 04018097. [[CrossRef](#)]
9. Valor, A.; Caleyó, F.; Hallen, J.M.; Velázquez, J.C. Reliability assessment of buried pipelines based on different corrosion rate models. *Corros. Sci.* **2013**, *66*, 78–87. [[CrossRef](#)]
10. Heidary, R.; Gabriel, S.A.; Modarres, M.; Groth, K.M.; Vahdati, N. A review of data-driven oil and gas pipeline pitting corrosion growth models applicable for prognostic and health management. *Int. J. Progn. Health Manag.* **2018**, *9*, 1–13. [[CrossRef](#)]
11. Ji, J.; Robert, D.; Zhang, C.; Zhang, D.; Kodikara, J. Probabilistic physical modelling of corroded cast iron pipes for lifetime prediction. *Struct. Saf.* **2017**, *64*, 62–75. [[CrossRef](#)]
12. Liu, W.; Wang, Z.; Liu, X.; Zeng, N.; Liu, Y.; Alsaadi, F.E. A survey of deep neural network architectures and their applications. *Neurocomputing* **2017**, *234*, 11–26. [[CrossRef](#)]
13. el Abbasy, M.S.; Senouci, A.; Zayed, T.; Mirahadi, F.; Parvizsedghy, L. Artificial neural network models for predicting condition of offshore oil and gas pipelines. *Autom. Constr.* **2014**, *45*, 50–65. [[CrossRef](#)]

14. Peng, S.; Zhang, Z.; Liu, E.; Liu, W.; Qiao, W. A new hybrid algorithm model for prediction of internal corrosion rate of multiphase pipeline. *J. Nat. Gas Sci. Eng.* **2021**, *85*, 103716. [[CrossRef](#)]
15. Seghier, M.E.A.B.; Keshtegar, B.; Taleb-Berrouane, M.; Abbassi, R.; Trung, N.-T. Advanced intelligence frameworks for predicting maximum pitting corrosion depth in oil and gas pipelines. *Process Saf. Environ. Prot.* **2021**, *147*, 818–833. [[CrossRef](#)]
16. Mazumder, R.K.; Salman, A.M.; Li, Y. Failure risk analysis of pipelines using data-driven machine learning algorithms. *Struct. Saf.* **2021**, *89*, 102047. [[CrossRef](#)]
17. Ossai, C.I. Corrosion defect modelling of aged pipelines with a feed-forward multi-layer neural network for leak and burst failure estimation. *Eng. Fail. Anal.* **2020**, *110*, 104397. [[CrossRef](#)]
18. Liu, Z.; Kleiner, Y. State of the art review of inspection technologies for condition assessment of water pipes. *Measurement* **2013**, *46*, 1–15. [[CrossRef](#)]
19. Hu, Z.; Tariq, S.; Zayed, T. A comprehensive review of acoustic based leak localization method in pressurized pipelines. *Mech. Syst. Signal Process.* **2021**, *161*, 107994. [[CrossRef](#)]
20. Bobrov, A.; Kuten, M. Intellectual innovations in acoustic emission control in the safety system of pipeline transport. *Transp. Res. Procedia* **2021**, *54*, 340–345. [[CrossRef](#)]
21. Li, S.; Wen, Y.; Li, P.; Yang, J.; Yang, L. Leak detection and location for gas pipelines using acoustic emission sensors. In Proceedings of the IEEE International Ultrasonics Symposium, Dresden, Germany, 7–10 October 2012; pp. 957–960. [[CrossRef](#)]
22. Smith, A.; Dixon, N.; Fowmes, G. Monitoring buried pipe deformation using acoustic emission: Quantification of attenuation. *Int. J. Geotech. Eng.* **2017**, *11*, 418–430. [[CrossRef](#)]
23. Bang, S.S.; Lee, Y.H.; Shin, Y. Defect detection in pipelines via guided wave-based time-frequency-domain reflectometry. *IEEE Trans. Instrum. Meas.* **2021**, *70*. [[CrossRef](#)]
24. Lowe, M.J.S.; Alleyne, D.N.; Cawley, P. Defect detection in pipes using guided waves. *Ultrasonics* **1998**, *36*, 147–154. [[CrossRef](#)]
25. Mohr, W.; Holler, P. On Inspection of Thin-Walled Tubes for Transverse and Longitudinal Flaws by Guided Ultrasonic Waves. *IEEE Trans. Sonics Ultrason.* **1976**, *23*, 369–373. [[CrossRef](#)]
26. Lowe, M.; Alleyne, D.; Cawley, P. Mode Conversion of Guided Waves by Defects in Pipes. In *Review of Progress in Quantitative Nondestructive Evaluation*; Springer: Boston, MA, USA, 1997; Volume 16. [[CrossRef](#)]
27. Hunaidi, O.; Chu, W.T. Acoustical characteristics of leak signals in plastic water distribution pipes. *Appl. Acoust.* **1999**, *58*, 235–254. [[CrossRef](#)]
28. Martini, A.; Rivola, A.; Troncossi, M. Autocorrelation analysis of vibro-acoustic signals measured in a test field for water leak detection. *Appl. Sci.* **2018**, *8*, 2450. [[CrossRef](#)]
29. Ghazali, M.F.; Beck, S.B.M.; Shucksmith, J.D.; Boxall, J.B.; Staszewski, W.J. Comparative study of instantaneous frequency based methods for leak detection in pipeline networks. *Mech. Syst. Signal Process.* **2012**, *29*, 187–200. [[CrossRef](#)]
30. Yang, M.D.; Su, N.C.; Pan, N.F.; Liu, P. Feature extraction of sewer pipe failures by wavelet transform and co-occurrence matrix. In Proceedings of the 2008 International Conference on Wavelet Analysis and Pattern Recognition, ICWAPR 2, Hong Kong, China, 30–31 August 2008. [[CrossRef](#)]
31. Cheraghi, N.; Taheri, F. A damage index for structural health monitoring based on the empirical mode decomposition. *J. Mech. Mater. Struct.* **2007**, *2*, 43–62. [[CrossRef](#)]
32. Moselhi, O.; Shehab-Eldeen, T. Classification of defects in sewer pipes using neural networks. *J. Infrastruct. Syst.* **2000**, *6*, 97–104. [[CrossRef](#)]
33. Carvalho, A.A.; Rebello, J.M.A.; Souza, M.P.V.; Sagrilo, L.V.S.; Soares, S.D. Reliability of non-destructive test techniques in the inspection of pipelines used in the oil industry. *Int. J. Press. Vessel. Pip.* **2008**, *85*, 745–751. [[CrossRef](#)]
34. Datta, D.; Sathish, S. Application of fractals to detect breast cancer. *J. Phys. Conf. Ser.* **2019**, *1377*, 012030. [[CrossRef](#)]
35. Hart, M.G.; Romero-Garcia, R.; Price, S.J.; Suckling, J. Global effects of focal brain tumors on functional complexity and network robustness: A prospective cohort study. *Clin. Neurosurg.* **2019**, *84*, 1201–1213. [[CrossRef](#)] [[PubMed](#)]
36. Dona, O.; Hall, G.B.; Noseworthy, M.D. Temporal fractal analysis of the rs-BOLD signal identifies brain abnormalities in autism spectrum disorder. *PLoS ONE* **2017**, *12*, e0190081. [[CrossRef](#)] [[PubMed](#)]
37. Babanin, O.; Bulba, V. Designing the technology of express diagnostics of electric train's traction drive by means of fractal analysis. *East.-Eur. J. Enterp. Technol.* **2016**, *4*, 45–54. [[CrossRef](#)]
38. Chandrasekaran, S.; Poomalai, S.; Saminathan, B.; Suthanthiravel, S.; Sundaram, K.; Hakkim, F.F.A. An investigation on the relationship between the hurst exponent and the predictability of a rainfall time series. *Meteorol. Appl.* **2019**, *26*, 511–519. [[CrossRef](#)]
39. Li, Q.; Liang, S.Y. Degradation trend prognostics for rolling bearing using improved R/S statistic model and fractional brownian motion approach. *IEEE Access* **2017**, *6*, 21103–21114. [[CrossRef](#)]
40. Hurst, H. Long Term Storage Capacity of Reservoirs. *Trans. Am. Soc. Civ. Eng.* **1951**, *116*, 770–799. [[CrossRef](#)]
41. Nazarychev, S.A.; Zagretdinov, A.R.; Ziganshin, S.G.; Vankov, Y.V. Classification of time series using the Hurst exponent. *J. Phys. Conf. Ser.* **2019**, *1328*, 012056. [[CrossRef](#)]
42. Khulief, Y.A.; Khalifa, A.; Mansour, R.B.; Habib, M.A. Acoustic detection of leaks in water pipelines using measurements inside pipe. *J. Pipeline Syst. Eng. Pract.* **2012**, *3*, 47–54. [[CrossRef](#)]
43. Martini, A.; Troncossi, M.; Rivola, A. Automatic leak detection in buried plastic pipes of water supply networks by means of vibration measurements. *Shock. Vib.* **2015**, *2015*, 165304. [[CrossRef](#)]